

*Electronic Supplementary Information*

**Bile acid-amino acid ester conjugates: Gelation, structural properties, and thermoreversible solid to solid phase transition**

Virpi Noponen,\* Nonappa, Manu Lahtinen, Arto Valkonen, Hannu Salo, Erkki Kolehmainen, and Elina Sievänen\*

*University of Jyväskylä, Department of Chemistry, P.O. Box 35, FIN-40014 University of Jyväskylä, Finland. E-mail: virpi.noponen@jyu.fi, elina.i.sievanen@jyu.fi; Fax: +358-14-260 2501*

**General procedures**

The starting materials used in the syntheses were purchased from commercial sources: lithocholic acid (Fluka,  $\geq 99\%$ ), deoxycholic acid (Aldrich, 98%), cholic acid (Aldrich, 98%), and L-methionine methyl ester hydrochloride (Aldrich, 98%). Triethylamine, ethyl chloroformate, and other reagents used in the synthetic steps as well as solvents used in chromatography were analytical grade reagents. 1,4-Dioxane was dried over Na prior to use. All chemicals were used without further purification.

Mass spectrometric measurements for compounds **1-3** were performed by using Micromass LCT time of flight (TOF) mass spectrometer with electrospray ionization (ESI) using positive ion mode. Controlling the LCT as well as acquiring and processing the data were performed with MassLynx NT software system. Flow rate of 30  $\mu\text{L}/\text{min}$  was used for the sample solution. The potentials of 55-82 and 4-5 V for the sample and extraction cones were applied. RF lens was set to a potential of 450-633 V and the potential in the capillary to 2900-3178 V. The desolvation temperature was set to 120  $^{\circ}\text{C}$  and the source temperature to 80  $^{\circ}\text{C}$ .

The synthetic route to **1-3** is described in Scheme S1. The mixed anhydride method used in the preparation of the target molecules and modified by us has been reported previously.<sup>1,2</sup>

**General procedure for the synthesis of bile acid-L-methionine methyl ester conjugates 1-3**

In a round-bottomed two-necked 100 mL flask bile acid (5 mmol, 1 eq) and 1,4-dioxane (42 mL) were cooled on an ice-water bath to +10 °C, after which triethylamine (6.7 mmol, 1.34 eq) was added to the solution from a dropping funnel, followed by a dropwise addition of ethyl chloroformate (6.7 mmol, 1.34 eq) in 1,4-dioxane (3 mL). The mixture was stirred at rt for 30 minutes. At the same time in another flask L-methionine methyl ester hydrochloride (6.7 mmol, 1.34 eq) was suspended in DMF (10 mL) at 0 °C, followed by a dropwise addition of triethylamine (6.7 mmol, 1.34 eq). The mixture was stirred at rt for 30 minutes. Then, L-methionine methyl ester in DMF was added dropwise to the freshly prepared activated bile acid, and stirring continued for 20 h at rt. The crude product obtained after the evaporation of the volatiles was dissolved in CHCl<sub>3</sub> (100 mL) and washed with water (2 x 75 mL), 0.1 M HCl solution (2 x 75 mL), water (2 x 75 mL), and finally with brine (2 x 75 mL). Organic layer was dried (Na<sub>2</sub>SO<sub>4</sub>), filtered, and the volatiles were evaporated under reduced pressure. The crude products were purified by column chromatography (silica gel, DCM:MeOH 94:6 for **1**, 90:10 for **2**, and 88:12 for **3**) to yield the compounds as colorless solid.

***N*-Lithocholyl-L-(methionine methyl ester) 1** (1.4 g, 53 %)

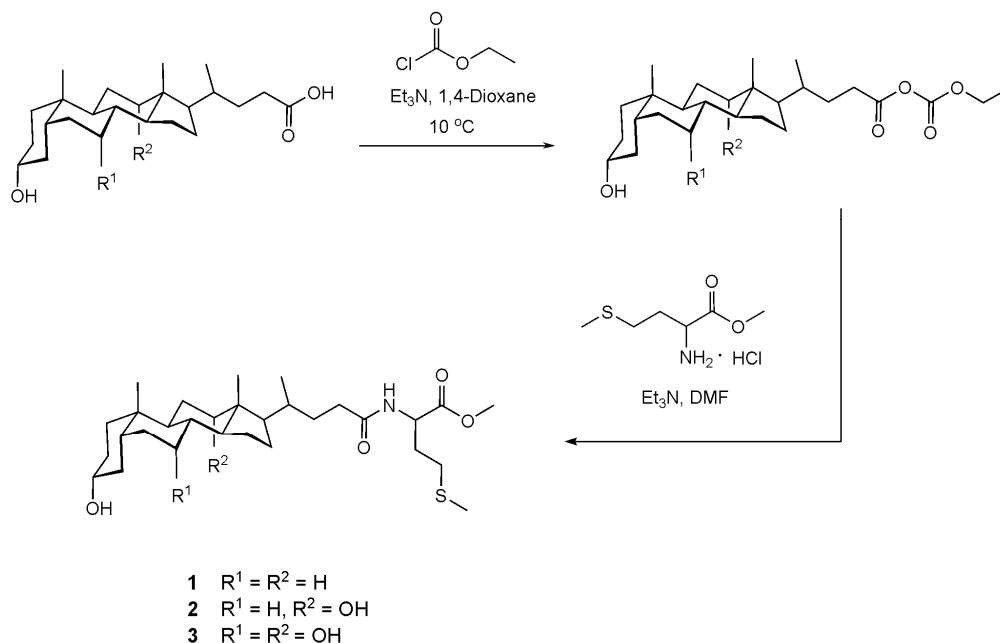
$\delta_{\text{H}}$  (500 MHz;  $\text{CDCl}_3$ ;  $\text{Me}_4\text{Si}$ ): 6.13 (1H, d, NH), 4.72 (1H, m, 25-CH), 3.75 (3H, s, COMe), 3.61 (1H, m, 3 $\beta$ -H), 2.50 (2H, m, 29-CH<sub>2</sub>), 2.28 (1H, m, 23 $\alpha/\beta$ -H), 2.09 (s, 3H, SMe), 0.92 (3H, d, 21-Me), 0.91 (3H, s, 19-Me), 0.63 (3H, s, 18-Me).  $\delta_{\text{C}}$  (126 MHz;  $\text{CDCl}_3$ ;  $\text{Me}_4\text{Si}$ ): 173.3 (C24), 172.6 (C26), 71.8 (C3), 56.47 (C17), 56.0 (C14), 52.5 (C27), 51.4 (C25), 42.7 (C13), 42.1 (C5), 40.4 (C9), 40.2 (C12), 36.4 (C4), 35.8 (C8), 35.4 (C20), 35.3 (C1), 34.6 (C10), 33.4 (C23), 31.8 (C28), 31.6 (C22), 30.5 (C2), 30.0 (C29), 28.2 (C7), 27.2 (C16), 26.4 (C6), 24.2 (C15), 23.3 (C19), 20.8 (C11), 18.3 (C21), 15.5 (C30), 12.0 (C18). ESI-TOF MS:  $[\text{M} + \text{Na}]^+ m/z = 544$ ,  $[\text{M} + \text{K}]^+ m/z = 560$ ,  $[2\text{M} + \text{Na}]^+ m/z = 1065$ . M.W. ( $\text{C}_{30}\text{H}_{51}\text{NO}_4\text{S}$ ) = 521.81. Elemental analysis: Found C, 68.72; H, 9.82; N, 2.64. Calc. for  $\text{C}_{30}\text{H}_{51}\text{NO}_4\text{S}$ : C, 69.05; H, 9.85; N, 2.68 %.

***N*-Deoxycholyl-L-(methionine methyl ester) 2** (2.2 g, 80 %)

$\delta_{\text{H}}$  (500 MHz;  $\text{CDCl}_3$ ;  $\text{Me}_4\text{Si}$ ): 6.18 (1H, d, NH), 4.72 (1H, m, 25-CH), 3.97 (1H, m, 12 $\beta$ -H), 3.75 (3H, s, COMe), 3.60 (1H, m, 3 $\beta$ -H), 2.50 (2H, m, 29-CH<sub>2</sub>), 2.30 (1H, m, 23 $\alpha/\beta$ -H), 2.09 (3H, s, SMe), 0.98 (3H, d, 21-Me), 0.90 (3H, s, 19-Me), 0.67 (3H, s, 18-Me).  $\delta_{\text{C}}$  (126 MHz;  $\text{CDCl}_3$ ;  $\text{Me}_4\text{Si}$ ): 173.3 (C24), 172.7 (C26), 73.1 (C12), 71.8 (C3), 52.5 (C27), 51.4 (C25), 48.3 (C14), 47.2 (C17), 46.5 (C13), 42.1 (C5), 36.5 (C4), 36.0 (C8), 35.2 (C1), 35.1 (C20), 34.1 (C10), 33.7 (C9), 33.3 (C23), 31.8 (C28), 31.4 (C22), 30.5 (C2), 30.0 (C29), 28.7 (C11), 27.5 (C16), 27.1 (C6), 26.1 (C7), 23.6 (C15), 23.1 (C19), 17.4 (C21), 15.5 (C30), 12.7 (C18). ESI-TOF MS:  $[\text{M} + \text{Na}]^+ m/z = 560$ ,  $[\text{M} + \text{K}]^+ m/z = 576$ ,  $[2\text{M} + \text{Na}]^+ m/z = 1097$ . M.W. ( $\text{C}_{30}\text{H}_{51}\text{NO}_5\text{S}$ ) = 537.81. Elemental analysis: Found C, 66.51; H, 9.34; N, 2.43. Calc. for  $\text{C}_{30}\text{H}_{51}\text{NO}_5\text{S} \cdot 0.25 \text{H}_2\text{O}$ : C, 66.44; H, 9.57; N, 2.58 %.

***N*-Cholyl-L-(methionine methyl ester) 3** (1.4 g, 50 %)

$\delta_{\text{H}}$  (500 MHz;  $\text{CDCl}_3$ ;  $\text{Me}_4\text{Si}$ ): 6.33 (1H, d, NH), 4.71 (1H, m, 25-CH), 3.97 (1H, m, 12 $\beta$ -H), 3.84 (1H, m, 7 $\beta$ -H), 3.75 (s, 3H, COMe), 3.45 (1H, m, 3 $\beta$ -H), 2.50 (2H, m, 29- $\text{CH}_2$ ), 2.09 (3H, s, SMe), 0.99 (3H, d, 21-Me), 0.89 (3H, s, 19-Me), 0.68 (3H, s, 18-Me).  $\delta_{\text{C}}$  (126 MHz;  $\text{CDCl}_3$ ;  $\text{Me}_4\text{Si}$ ): 173.6 (C24), 172.7 (C26), 73.0 (C12), 72.0 (C3), 68.4 (C7), 52.5 (C27), 51.5 (C25), 46.8 (C17), 46.5 (C13), 41.9 (C14), 41.5 (C5), 39.7 (C4), 39.6 (C8), 35.3 (C1), 35.2 (C20), 34.7 (C10), 34.7 (C6), 33.1 (C23), 31.8 (C28), 31.4 (C22), 30.5 (C2), 30.1 (C29), 28.3 (C11), 27.5 (C16), 26.6 (C9), 23.2 (C15), 22.5 (C19), 17.5 (C21), 15.5 (C30), 12.5 (C18). ESI-TOF MS:  $[\text{M} + \text{Na}]^+ m/z = 576$ ,  $[2\text{M} + \text{Na}]^+ m/z = 1129$ . M.W. ( $\text{C}_{30}\text{H}_{51}\text{NO}_6\text{S}$ ) = 553.81. Elemental analysis: Found C, 64.95; H, 9.27; N, 2.42. Calc. for  $\text{C}_{30}\text{H}_{51}\text{NO}_6\text{S}$ : C, 65.06; H, 9.28; N, 2.53 %.



**Scheme S1** Synthetic route leading to compounds **1-3**.

### **General procedures for gelation studies, SEM, and NMR spectroscopy**

Gelation tests for compounds **1-3** were conducted by weighing 5 mg of a particular compound in a test tube and adding 500  $\mu\text{L}$  of the solvent in question. The obtained mixture was heated until it turned into a clear solution. The solution was allowed to attain room temperature or sonicated for 1 minute, and observations with regard to gelation were made after that. The state of the material was examined by the “stable-to-inversion of a test tube”-method. If no flow was determined, the material was defined to be a gel, denoted by “G” in Table 1. In some cases the gel seemed to be fairly weak, and this is denoted by “G-“. All non-gelator containing tubes were left at ambient temperature and possible crystallization was monitored within days or weeks.

Scanning electron micrographs were taken with Bruker Quantax400 EDS microscope equipped with a digital camera. Samples of the xerogels were prepared by placing a hot, clear solution of the gelator in toluene on carbon tape placed over a sample stub, and after evaporation of the solvent, coated with gold in a JEOL Fine Coat Ion Sputter JFC-1100.

VT  $^1\text{H}$  NMR spectra, as well as the routine NMR spectra used for characterization of the prepared compounds were recorded with a Bruker Avance DRX 500 MHz spectrometer operating at 500.13 MHz ( $^1\text{H}$ ) and 125.77 MHz ( $^{13}\text{C}$ ), respectively. The  $^1\text{H}$  NMR chemical shifts are referenced to the signal of residual  $\text{CHCl}_3$  (7.26 ppm from TMS) or  $\text{C}_6\text{H}_6$  (7.16 ppm from TMS). The  $^{13}\text{C}$  NMR chemical shifts are referenced to the centre peak of the solvent  $\text{CDCl}_3$  (77.0 ppm from TMS). A composite pulse decoupling, Waltz-16, has been used to remove proton couplings from  $^{13}\text{C}$  NMR spectra.  $^{13}\text{C}$  CPMAS NMR

spectra of the gels and the solid state samples were recorded at room temperature with Bruker Avance 400 MHz spectrometer equipped with a CPMAS probe, using 4 mm ZrO<sub>2</sub> rotors or 12  $\mu$ L HR MAS rotor (2 % (w/v) benzene gel of compound **1**). The solid samples were spun at rates of 8 or 10 kHz and the gel samples at 4 or 5 kHz. The CP contact time was 2 or 4 ms and relaxation delay 2, 4, or 5 s depending on the measurement.

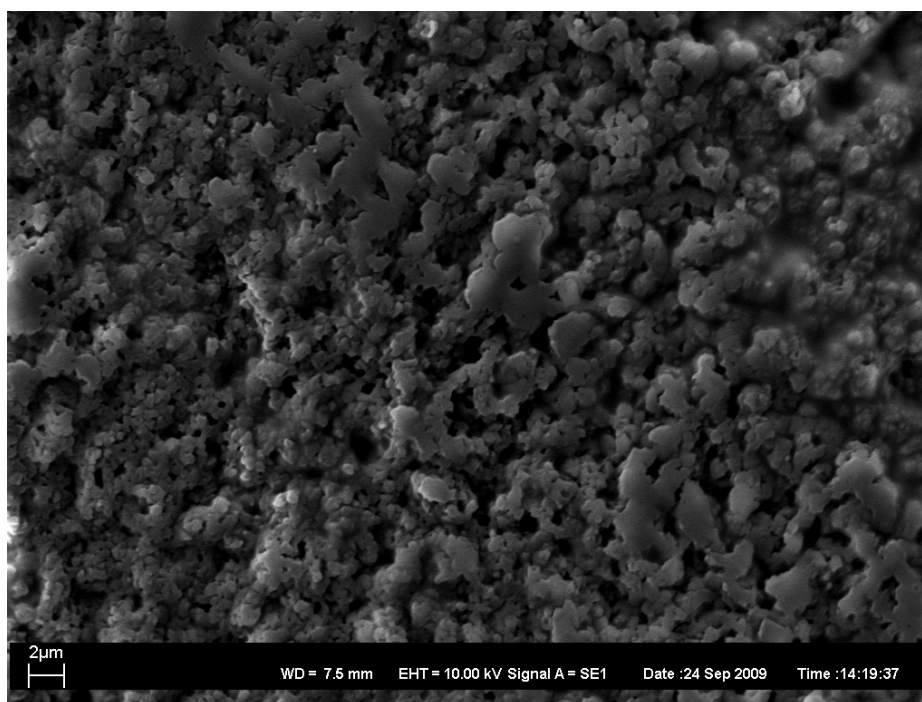


**Figure S1** SEM image of the xerogel of **3** in toluene (4 % w/v).

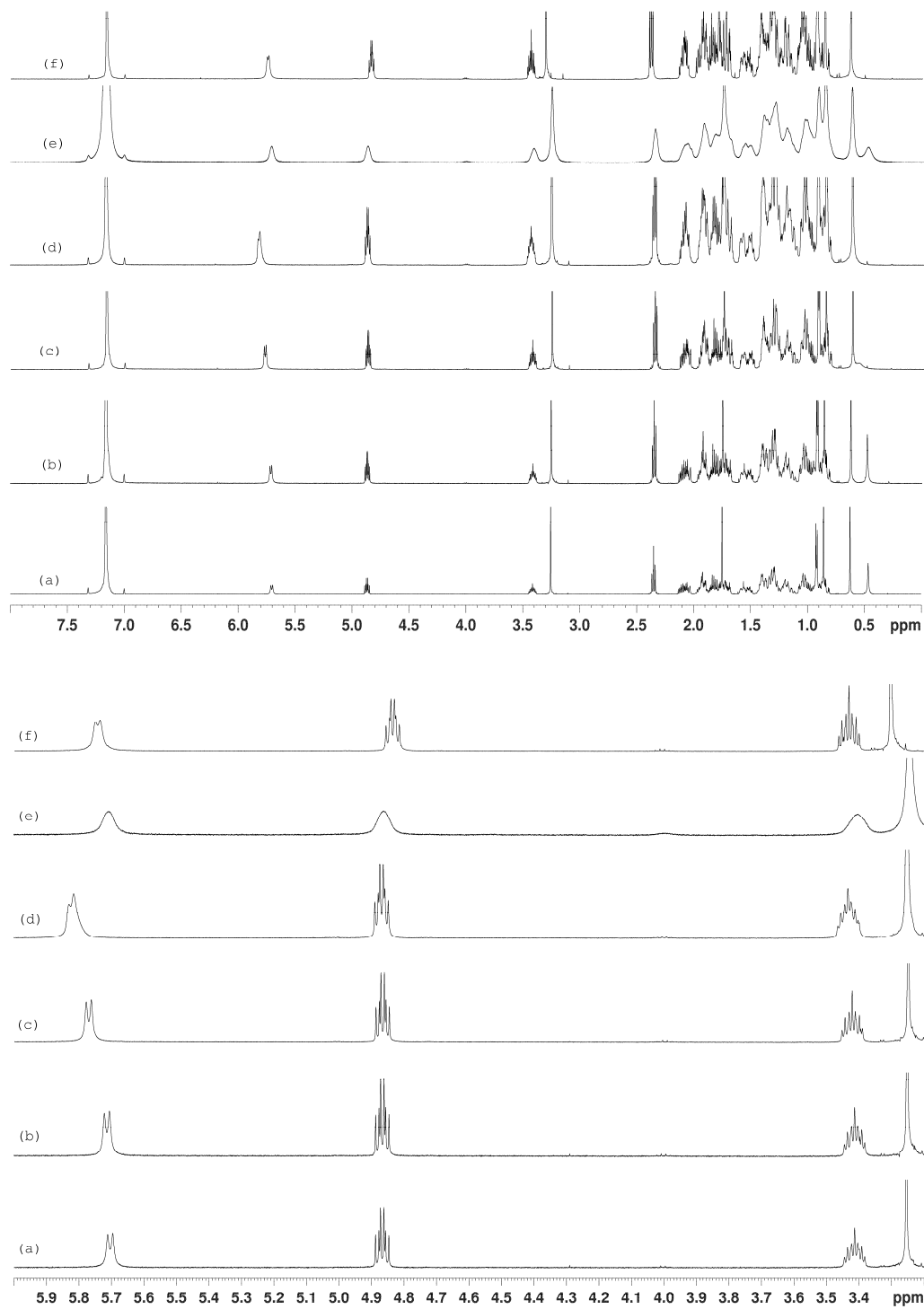


**Figure S2** Concentration-dependent  $^1\text{H}$  NMR of **1** in benzene- $\text{d}_6$ . (a) 0.25 % (4.8 mM); (b) 0.50 %; (c) 1.0 %; (d) 1.5 %; (e) 2.0 % (gel) at 30 °C and (f) 2.0 % at 60 °C.

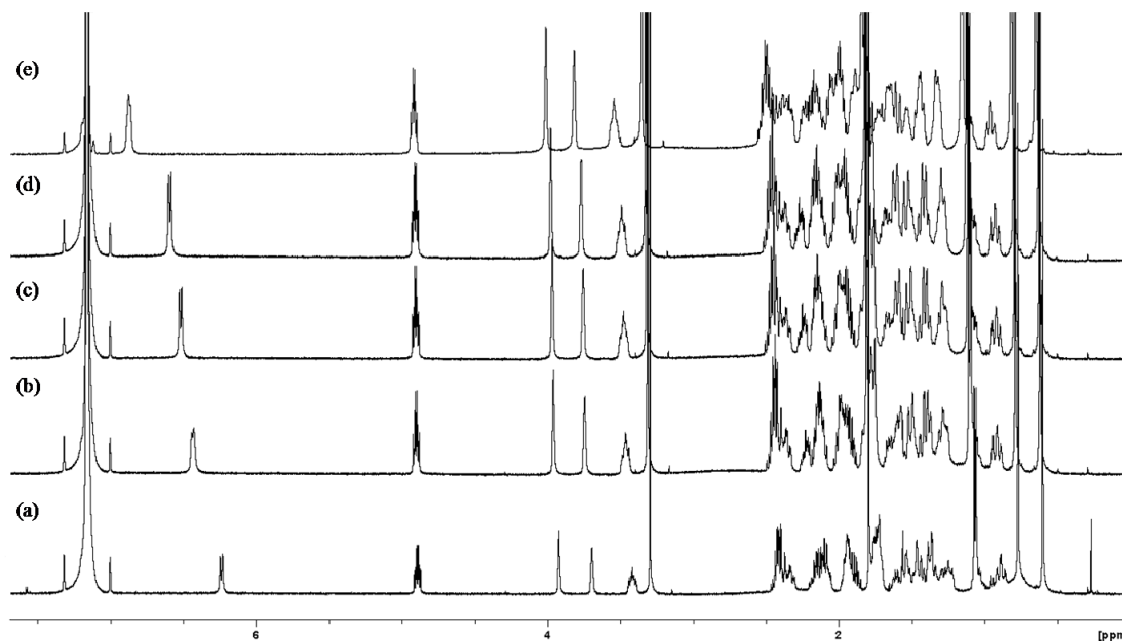


**Figure S3** Concentration-dependent  $^1\text{H}$  NMR of **3** in benzene- $d_6$ .  
(a) 0.25 % (4.5 mM); (b) 0.50 %; (c) 0.75 %; (d) 1.0 %; (e) 2.0 % at 30 °C.

## X-ray crystallography

### Single crystal X-ray analysis

Crystals suitable for single crystal X-ray analysis were grown from MeOH (for **1**), *t*-butylbenzene (**2**), and ethyl acetate (**3**) by slow evaporation. For all three structure determinations the single crystal was mounted on a Bruker-Nonius KappaCCD diffractometer equipped with an APEX-II area detector and an Oxford Cryosystems 600 N<sub>2</sub> cooling device, using graphite-monochromated Mo-K $\alpha$  radiation. COLLECT<sup>3a</sup> software was used in data collection, DENZO-SMN<sup>3b</sup> in cell refinement and data reduction, SIR-2002<sup>3c</sup> (for **1**) or SIR-2004<sup>3d</sup> in structure solution, and SHELXL-97<sup>3e</sup> in structure refinement on  $F^2$ . Absorption correction was not applied. Crystal data and selected structural parameters for compounds **1-3** are presented in Tables S1 and S2, respectively.



**Table S1** Crystallographic data and refinement parameters of **1-3**

| Comp.  | <b>1</b>  | <b>1b</b>   | <b>2</b>  | <b>3</b>  |
|--|---|---|---|---|
| formula  | C <sub>30</sub> H <sub>51</sub> NO <sub>4</sub> S               | C <sub>30</sub> H <sub>51</sub> NO <sub>4</sub> S | C <sub>30</sub> H <sub>51</sub> NO <sub>5</sub> S               | C <sub>30</sub> H <sub>51</sub> NO <sub>6</sub> S               |
| formula weight (g mol <sup>-1</sup> )            | 521.78  | 521.80  | 537.78  | 553.78  |
| temp (°C)  | -150  | 25  | -150  | -150  |
| wavelength (Å)                                   | 0.71073   | 1.5406  | 0.71073   | 0.71073   |
| crystal system                                   | monoclinic  | monoclinic  | monoclinic  | monoclinic  |
| space group (No.)                                | <i>P</i> 2 <sub>1</sub> (4)                                     | <i>P</i> 2 <sub>1</sub> (4)                       | <i>P</i> 2 <sub>1</sub> (4)                                     | <i>P</i> 2 <sub>1</sub> (4)                                     |
| unit cell dimensions                             |   |   |   |   |
| <i>a</i> (Å)                                     | 9.9056(3)   | 10.1039(3)  | 10.1765(4)  | 10.2484(3)  |
| <i>b</i> (Å)                                     | 7.6387(3)   | 7.5996(2)   | 7.5262(3)   | 7.5897(2)   |
| <i>c</i> (Å)                                     | 19.5268(6)  | 19.6508(5)  | 19.5268(8)  | 19.3681(5)  |
| $\beta$ (°)                                      | 104.788(2)  | 101.655(2)  | 102.747(2)  | 105.323(2)  |
| volume (Å <sup>3</sup> )                         | 1428.57(8)  | 1477.78(7)  | 1458.70(10)   | 1452.94(7)  |
| <i>Z</i>   | 2   | 2   | 2   | 2   |
| $\rho_{calc}$ (Mg/m <sup>3</sup> )               | 1.213   |   | 1.224   | 1.266   |
| $\mu$ (mm <sup>-1</sup> )                        | 0.148   |   | 0.150   | 0.155   |
| <i>F</i> (000)                                   | 572   |   | 588   | 604   |
| crystal size (mm <sup>3</sup> )                  | 0.30 × 0.16 × 0.05  | powder  | 0.22 × 0.07 × 0.03  | 0.25 × 0.10 × 0.08  |
| $\theta$ range (°)                               | 2.13 - 25.50  | 3-75 <sup>a</sup>                                 | 2.51 - 27.50  | 2.57 - 27.50  |
| step size (°)                                    |   | 0.008 <sup>a</sup>                                |   |   |
| index ranges                                     | -11 ≤ <i>h</i> ≤ 12<br>-9 ≤ <i>k</i> ≤ 9<br>-23 ≤ <i>l</i> ≤ 22 |   | -13 ≤ <i>h</i> ≤ 13<br>-9 ≤ <i>k</i> ≤ 9<br>-25 ≤ <i>l</i> ≤ 25 | -13 ≤ <i>h</i> ≤ 13<br>-9 ≤ <i>k</i> ≤ 9<br>-25 ≤ <i>l</i> ≤ 25 |
| No. of profile data steps                        |   | 8998  |   |   |
| No. of reflections                               | 8897  | 970   | 6520  | 6560  |
| independent refl. / <i>R</i> <sub>int</sub>      | 5294 / 0.0532   | 970 / -   | 3614 / 0.0962   | 3580 / 0.0571   |
| completeness to $\theta$                         | 99.9  |   | 99.9  | 99.8  |
| Restraints / parameters                          | 3 / 331   |   | 52 / 353  | 5 / 355   |
| Goof (on <i>F</i> <sup>2</sup> )                 | 1.055   | 1.24 <sup>b</sup>                                 | 1.068   | 1.066   |
| No. of all variables                             |   | 131 (278) <sup>c</sup>                            |   |   |
| No. profile variables                            |   | 12  |   |   |
| <i>R</i> <sub>p</sub>                            |   | 0.109 <sup>d</sup>                                |   |   |
| <i>R</i> <sub>wp</sub>                           |   | 0.113   |   |   |
| <i>R</i> <sub>c</sub>                            |   | 0.101   |   |   |
| <i>R</i> <sub>F</sub>                            |   | 0.0452  |   |   |
| <i>R</i> <sub>B</sub>                            |   | 0.0395  |   |   |
| Final <i>R</i> indices                           | <i>R</i> 1 = 0.0568   |   | <i>R</i> 1 = 0.0719   | <i>R</i> 1 = 0.0553   |
| [ <i>I</i> > 2 $\sigma$ ( <i>I</i> )]            | w <i>R</i> 2 = 0.1040   |   | w <i>R</i> 2 = 0.1090   | w <i>R</i> 2 = 0.1025   |
| <i>R</i> indices (all data)                      | <i>R</i> 1 = 0.0770   |   | <i>R</i> 1 = 0.1282   | <i>R</i> 1 = 0.0763   |
|  | w <i>R</i> 2 = 0.1134   |   | w <i>R</i> 2 = 0.1297   | w <i>R</i> 2 = 0.1117   |
| Absolute structure parameter                     | -0.03(11)   |   | - <sup>e</sup>  | - <sup>e</sup>  |
| Largest diff. peak and hole (e./Å <sup>3</sup> ) | 0.258 and -0.219  |   | 0.291 and -0.328  | 0.282 and -0.275  |

<sup>a</sup> 2 $\theta$ , in case of powder diffraction. <sup>b</sup> goodness-of-fit on  $\chi^2$ . <sup>c</sup> when all hydrogen atom positions were included. <sup>d</sup> all agreement factors are background corrected. <sup>e</sup> meaningless Flack parameter removed, Friedel-pairs merged.

**Table S2** Selected structural parameters of **1-3**

|   | <b>1</b><br>(-150 °C) | <b>1b</b><br>(+25 °C) | <b>2</b>              | <b>3</b>              |
|---|-----------------------|-----------------------|-----------------------|-----------------------|
| $\langle(\text{C13-C17-C20-C22}) / ^\circ$    | 176.1(3)              | 175(1)                | 170.3(4)              | -179.0(3)             |
| $\langle(\text{C17-C20-C22-C23}) / ^\circ$    | -169.2(3)             | -175(1)               | -173.3(4)             | -172.4(3)             |
| $\langle(\text{C20-C22-C23-C24}) / ^\circ$    | 174.1(3)              | 156(1)                | 167.2(4)              | 176.1(3)              |
| $\langle(\text{C22-C23-C24-N24}) / ^\circ$    | 116.1(3)              | 128(2)                | 133.5(5)              | 116.9(4)              |
| $\langle(\text{C25-C28-C29-S1}) / ^\circ$     | 172.9(2)              | -155(1)               | -160.2(4)             | 177.3(3)              |
| $\langle(\text{C28-C29-S1-C30}) / ^\circ$     | 74.6(3)               | 118(1)                | -170.8(5)             | 73.3(3)               |
| $d(\text{O3}\cdots\text{O24}) / \text{\AA}$   | 2.902(4) <sup>a</sup> | 3.04(3) <sup>e</sup>  | 2.846(6) <sup>b</sup> | 2.868(4) <sup>c</sup> |
| $d(\text{N24}\cdots\text{O3}) / \text{\AA}$   | 3.184(4) <sup>a</sup> | 3.33(3) <sup>e</sup>  | 3.233(6) <sup>b</sup> | 3.230(5) <sup>c</sup> |
| $d(\text{O7}\cdots\text{O12}) / \text{\AA}$   | -                     | -                     | -                     | 3.124(4) <sup>d</sup> |
| $\langle(\text{O3}\cdots\text{O24}) / ^\circ$ | 165(4) <sup>a</sup>   | 156(1) <sup>e</sup>   | 170(7) <sup>b</sup>   | 169(5) <sup>c</sup>   |
| $\langle(\text{N24}\cdots\text{O3}) / ^\circ$ | 166(3) <sup>a</sup>   | 145(10) <sup>e</sup>  | 161(5) <sup>b</sup>   | 159(4) <sup>c</sup>   |
| $\langle(\text{O7}\cdots\text{O12}) / ^\circ$ | -                     | -                     | -                     | 158(4) <sup>d</sup>   |

Symmetry operations: <sup>a</sup>-x+2,y+1/2,-z+2; <sup>b</sup>-x+1,y-1/2,-z+1; <sup>c</sup>-x+1,y-1/2,-z+1; <sup>d</sup>

-x+1,y+1/2,-z+1; <sup>e</sup>1-x, -1/2+y, -z

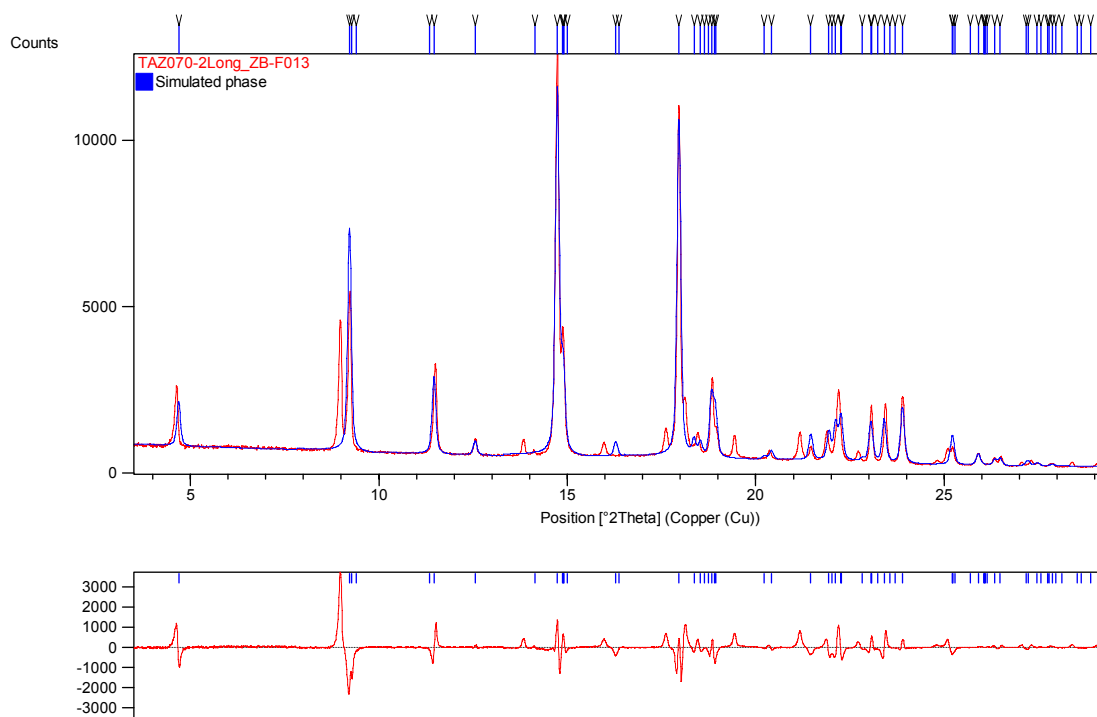


**Figure S4** Le Bail fit of **1b** using structure parameters of the low-temperature structure **1**. Solid red line represents experimental data and blue line calculated data. The difference plot is placed at the bottom. The few unindexed peaks can clearly be seen for example at 8.97°, 13.83°, 15.97° and 19.43° in 2θ, as well as misfit of peaks at 4.7°, 9.2° and 11.5° 2θ.

### **X-ray powder diffraction at ambient and non-ambient conditions**

The xerogel sample for powder X-ray diffraction studies was obtained by placing a 4 % (w/v) hot solution of compound **1** in toluene on a glass plate, and allowing it to dry for two days at ambient temperature. The xerogel sample was then scratched from the glass plate and taken for measurements. The X-ray powder diffraction data was measured with PANalytical X'Pert PRO diffractometer in Bragg–Brentano geometry using step–scan technique and incident beam Johansson monochromator to produce pure Cu-K $\alpha_1$  radiation (1.5406 Å; 45kV, 40mA). For low-temperature measurements the default sample stage was changed to an Anton Paar TTK 450 chamber with automated sample-stage height-controller, vacuum pump system and liquid N<sub>2</sub> cooling unit. The diffraction data was collected by X'Celerator detector using continuous scanning mode in 2 $\theta$  range of 3–75° with a step size of 0.008° and a counting time of 700 s per step for room temperature data. A 2 $\theta$  range of 3–60° with a step size of 0.033° and a counting time of 80 s per step was used for temperature-dependent measurements. Programmable divergence slit (PDS) was used for all measurements in automatic mode to set irradiated length on sample to 10 mm together with fixed 10 mm incident beam mask (7 mm and 10 mm, respectively for non-ambient). Soller slits of 0.02° were used on incident and diffracted beam sides together with anti-scatter slits of 4° and 13 mm (4° and 6.6 mm for non-ambient conditions), respectively.

Lightly hand-ground powder sample was prepared on a silicon-made zero-background holder using petrolatum jelly as an adhesive, in a case of conventional measurement. For non-ambient measurements the sample was prepared into a TTK 450 chamber and cooled under vacuum (0.129 mbar) from +25 to -150 °C with a rate of 10

°C/min by controlled liquid N<sub>2</sub> cooling. Diffraction patterns were recorded isothermally at temperatures of +25, -50, -100, and -150 °C and finally again at +25 °C. All data were converted from automatic slit mode (ADS) to the fixed slit mode (FDS) data in X'pert HighScore Plus v. 2.2d software before further analyses. The simulated XRD pattern used for comparison purposes was generated by the program Mercury<sup>4</sup> using the CIF of the single crystal structure presented in this study.

### **Powder structure determination**

Powder structure determination for room-temperature structure **1b** including data processing, indexing (DICVOL04)<sup>5</sup>, space group determination, structure solving by simulating annealing method, and a rigid-body Rietveld refinement were made using program DASH 3.1<sup>6</sup> and the final Rietveld refinement with full 2 $\theta$  range by FULLPROF v4.70<sup>7</sup>. The final Rietveld refinement plot can be seen in the main text (Fig. 9). The first 21 diffraction peak positions were used as an input for the auto-indexing procedure made by DICVOL04. The solution having all the peaks indexed in a monoclinic unit cell  $a = 10.1039(3)$ ,  $b = 7.5996(2)$ ,  $c = 19.6508(5)$  Å and  $\beta = 101.655(2)^\circ$  with high figure of merits ( $M_{21} = 72$ ,  $F_{21} = 220$  (0.0032, 30))<sup>8</sup> was repeatedly resulted. Similar unit cell settings were acquired by comparative auto-indexing in X'pert HighScore Plus using programs TREOR<sup>9</sup> and McMaille<sup>10</sup>. Based on the extinction rules and chirality of the molecule ruling out the centrosymmetric space group settings, the polar  $P2_1$  space group was assigned. The final unit cell refinement with the  $P2_1$  space group resulted an excellent Pawley fit indicating correctness of the determined cell settings and space group ( $R_{wp} = 0.0918$  and Pawley  $\chi^2 = 1.11$ ).

The structure determination was made with DASH program that is based on simulated annealing method in which known structure moiety/moieties are needed to the structure determination. For **1b**, the entire conjugate molecule with hydrogen atoms was used as a moiety and was first imported to the molecular editor program Avogadro v 0.9.7<sup>11</sup> using available CIF of the single crystal structure as a basis of the structure model. Optimized geometry of the built molecule was produced by molecular mechanics in Avogadro from which the *Z*-matrices for the DASH program was then generated. During structure determination the translation of the centre of mass of the molecule along *y*-axis was fixed (0.5, 0.5 and 0.5) due to polar space group *P2*<sub>1</sub>. Other translational and rotational variables were allowed to refine freely. More than dozen simulating annealing runs were made each having  $10 \times 10^6$  moves, and  $\sim 75$  % of the runs ended up to the same structure model; the best fits having profile  $\chi^2$  between 10.41 – 13.43 %. Rigid-body Rietveld refinement implemented in DASH was carried out with the best structure model, improving the profile  $\chi^2$  to 4.29.

The final Rietveld refinement was made with full  $2\theta$  range using program FULLPROF in which lattice, profile, and interpolated background parameters together with zero-offset, scale factor, atomic coordinates, and isotropic temperature factors of all non-hydrogen atoms were refined. For background, 20 refined points were used at first, which positions were then set fixed with initiation of interpolation (cubic spline) between the background points. Pseudo-Voigt function was used for the peak profiles and uniform isotropic temperature factor was refined for each non-hydrogen atom type and a single fixed isotropic temperature factor ( $U = 0.076$ ) was used for all hydrogen atoms.

In a final stage of the refinement soft distance restraints (129) were applied, to maintain proper molecular geometry by allowing measured atom distances less than 2.0 Å to vary within 0.02 Å while atom coordinates were refined. Three angle restraints (allowed to vary 1.0°) were introduced to the amide group and in addition, hydrogen atoms of hydroxyl (O3) and amide (N24) groups were allowed to refine freely. Finally, to evaluate the influence of using fixed hydrogen atoms in the refinement, few refinement steps were made by freeing all hydrogen positions. As expected, the hydrogen atoms started to distort out from their ideal positions (see Figure S3 for comparison). However, all the non-hydrogen atoms still remain in their previously refined positions indicating that the final refinement with the applied soft restraints and fixed hydrogen atoms yields realistic structure model. The comparison of the structure models obtained by the rigid-body Rietveld refinement (DASH) and whole-pattern refinement using FULLPROF reveals that the acceptable structure model can already be obtained by the constrained refinement as the changes on further refinement stages are only minor (Fig. S3).

The instrumental resolution of the equipment was determined using highly crystalline silicon standard (SRM 640b, National Institute of Standards & Technology). For silicon standard, the sharpest full-width at half-maximum (FWHM) of 0.04° (2θ) was obtained on diffraction peak at 28.44° (2θ). The instrument was calibrated using the silicon standard so that an absolute error of less than 0.01° (2θ) on peak positions was achieved.

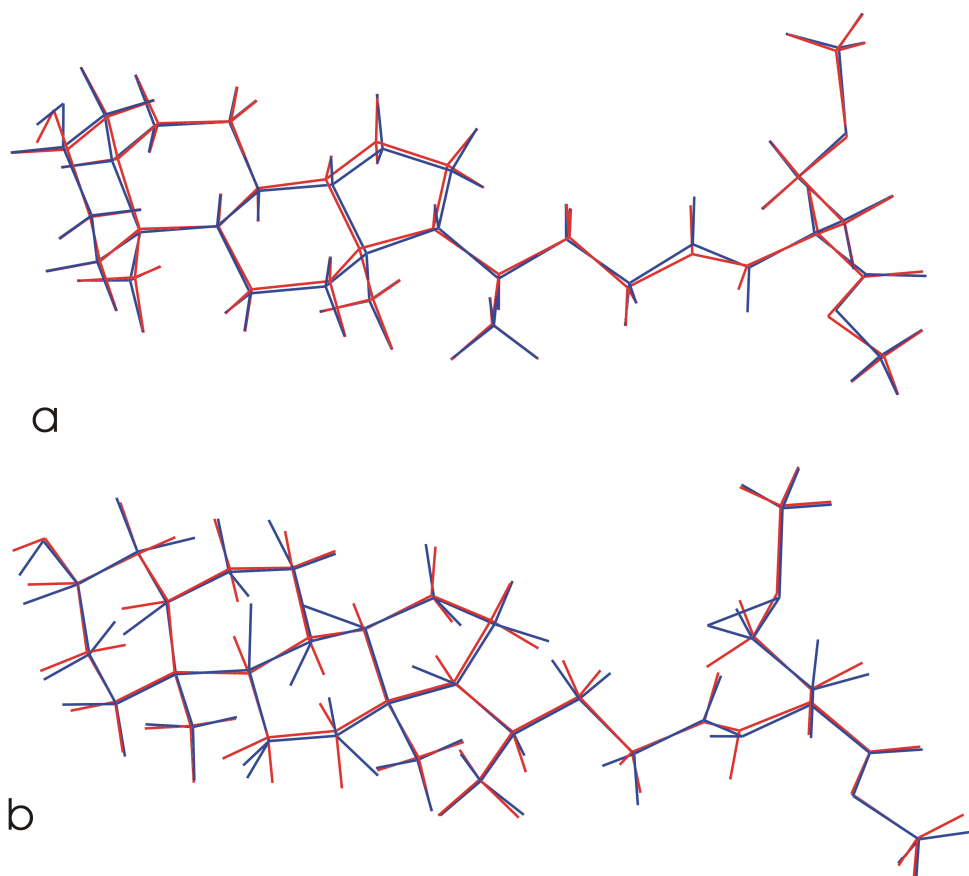


**Figure S5** Overlay of structure models of **1b**: a) final structure model (red) compared to the structure model after rigid-body Rietveld refinement (blue); b) structure model refined with fixed hydrogen atoms (red) compared to model with all atom positions refined (blue).

## References

- 1 S. Bergstrom and A. Norman, *Acta Chem. Scand.*, 1953, **7**, 1126–1127.
- 2 V. Noponen, S. Bhat, E. Sievänen and E. Kolehmainen, *Mater. Sci. Eng., C*, 2008, **28**, 1144–1148.
- 3 (a) COLLECT data collection software, Bruker AXS, Delft, The Netherlands, 2008; (b) Z. Otwinowski and W. Minor, in *Methods Enzymol.*, Vol. 276: *Macromolecular Crystallography*, Part A, ed. C. W. Carter Jr. and R. M. Sweet, Academic Press, New

- York, 1997, pp. 307–326; (c) M. C. Burla, M. Camalli, B. Carrozzini, G. L. Cascarano, C. Giacovazzo, G. Polidori and R. Spagna, *J. Appl. Crystallogr.*, 2003, **36**, 1103; (d) M. C. Burla, R. Caliendo, M. Camalli, B. Carrozzini, G. L. Cascarano, L. De Caro, C. Giacovazzo, G. Polidori and R. Spagna, *J. Appl. Crystallogr.*, 2005, **38**, 381–388; (e) G. M. Sheldrick, *Acta Crystallogr., Sect. A*, 2008, **64**, 112–122.
- 4 C. F. Macrae, P. R. Edgington, P. McCabe, E. Pidcock, G. P. Shields, R. Taylor, M. Towler and J. van de Streek, MERCURY, v2.3, *J. Appl. Crystallogr.*, 2006, **39**, 453–457.
- 5 A. Boulif and D. Louër, *J. Appl. Crystallogr.*, 2004, **37**, 724–731.
- 6 W. I. F. David, K. Shankland, J. van de Streek, E. Pidcock, W. D. S. Motherwell, J. C. Cole, *J. Appl. Crystallogr.*, 2006, **39**, 910–915.
- 7 J. Rodriguez-Carvajal, FULLPROF: A Program for Rietveld Refinement and Pattern Matching Analysis, Abstracts of the Satellite Meeting on Powder Diffraction of the XV Congress of the IUCr, Toulouse, France, 1990, 127.
- 8 P. M. De Wolff, *J. Appl. Crystallogr.*, 1986, **1**, 108–113.
- 9 P.E. Werner, L. Erikson and M. Westdahl, *J. Appl. Crystallogr.*, 1985, **18**, 367–370.
- 10 A. Le Bail, *Powder Diffraction*, 2004, **19**, 249–254.
- 11 Avogadro 0.9.7., [http://avogadro.openmolecules.net/wiki/Main\\_Page](http://avogadro.openmolecules.net/wiki/Main_Page), 2009.